Optical mapping of effective brain networks during the tangram task

Zhishan Hu, Keng-Fong Lam, Zhen Yuan

Zhishan Hu, Keng-Fong Lam, Zhen Yuan, "Optical mapping of effective brain networks during the tangram task," Proc. SPIE 11225, Clinical and Translational Neurophotonics 2020, 1122507 (17 February 2020); doi: 10.1117/12.2542229

SPIE.

Event: SPIE BiOS, 2020, San Francisco, California, United States

Optical mapping of effective brain networks during the tangram task

Zhishan Hu[1,2,] Keng-Fong Lam[1,2,], Zhen Yuan[1,2,*]

[1] Centre for Cognition and Brain Sciences, University of Macau, Macau SAR, China

[2] Faculty of Health Sciences, University of Macau, Macau SAR, China

***Corresponding Author**:

Dr. Zhen Yuan (Professor): Email: zhenyuan@um.edu.mo

Abstract. Although the neural basis underlying visuospatial reasoning has been widely explored by neuroimaging techniques, the brain activation patterns during naturalistic visuospatial reasoning such as tangram remains unclear. In this study, the directional functional connectivity of fronto-parietal networks during the tangram task was carefully inspected by using combined functional near-infrared spectroscopy (fNIRS) and conditional Granger causality analysis (GCA). Meanwhile, the causal networks during the traditional spatial reasoning task were also characterized to exhibit the differences with those during the tangram task. We discovered that the tangram task in a natural environment showed enhanced activation in the fronto-parietal regions, particularly the frontal cortex. In addition, a strong directional connectivity from the right prefrontal cortex to left angular gyrus was detected for the complex spatial reasoning condition of spatial reasoning task, whereas no effective connectivity was identified between the frontal and parietal cortices during the tangram task. Further correlation analyses showed that the behavioral performance in the spatial reasoning rather than the tangram task manifested the relationship with the connectivity between the frontal and parietal cortex. Our findings demonstrate that the tangram task measures a different aspect of the visuospatial reasoning ability which requires more trial-and-error strategies and creative thinking rather than inductive reasoning. In particular, the frontal cortex is mostly involved in tangram puzzle-solving, whereas the interaction between frontal and parietal cortices might be disrupted by the hands-on experience during the tangram task. Our study also indicates that conditional GCA combined with fNIRS neuroimaging technique is a robust tool for constructing the causal networks associated with natural visuospatial reasoning, which paves a new avenue for an improved understanding of the neural mechanism underlying tangram.

Keywords: tangram; visuospatial reasoning; Granger causality; fNIRS; brain networks

Clinical and Translational Neurophotonics 2020, edited by Steen J. Madsen, Victor X. D. Yang, Nitish V. Thakor
Proc. of SPIE Vol. 11225, 1122507 · © 2020 SPIE · CCC code: 1605-7422/20/$21 · doi: 10.1117/12.2542229

1. Introduction

Tangram is an ancient Chinese puzzle that requires putting together seven flat shapes to form a specific shape. To date, the neural underpinnings underlying tangram puzzle-solving remain unclear.

Recent neuroimaging studies showed that enhanced cortical activation was detected in the prefrontal cortex during the tangram tasks rather than during the control task that merely requested participants to match the tangram pieces to given shapes.[1,2] In addition, it was discovered that cortical activation in the frontal cortex was regulated by the task difficulty and participants' performance. Further, previous studies also demonstrated that cortical activation in the prefrontal cortex was mainly due to the cognitive processing of visuospatial reasoning. However, according to the well-recognized parieto-frontal integration theory (P-FIT), the parietal cortex also plays an essential role in visuospatial reasoning .[3] For example, the right superior parietal lobule (SPL) including the somatosensory association cortex (SAC) is involved in attention processing, whereas the left homologue is related to the memorization and manipulation of visual stimuli[4] and the rostrolateral prefrontal cortex (RLPFC) and inferior parietal lobule/sulcus (IPL/IPS) are engaged in visuospatial relational reasoning. More specifically, it was discovered that the left IPL was associated with the spatial perception and visuomotor integration. Meanwhile, the bilateral angular gyrus (AG) as part of IPL, is associated with the spatial analysis of sensory inputs and mental representations while the function of right AG is essential for spatial cognition 13). Importantly, the RLPFC also exhibits significant correlation with multiple high-level cognitive functions such as planning, managing completing goals, integrating information, and rapid learning of novel rules.

In addition to cortical activation, functional connectivity (FC) in the fronto-parietal networks is considered to be pivotal to visuospatial reasoning.[5] For example, previous work highlighted that increased activity in the fronto-parietal networks (primarily the RLPFC and IPS) was a potential neural substrate for complex visuospatial reasoning.[5] In addition, enhanced FC in the lateral fronto-parietal networks was also discovered to be associated with reasoning including visuospatial reasoning.[6]

Although the neural basis underlying visuospatial reasoning was explored previously, seldom studies have been carried out to inspect cortical activation and neural networks associated with naturalistic visuospatial reasoning such as tangram. Given that the functions of prefrontal and parietal cortices are the neuropsychological basis of visuospatial reasoning, it is critical to examine the relationship between the activity of fronto-parietal networks and tangram puzzle-solving. In this study, it is hypothesized that the effective connectivity between the frontal and parietal cortices can be detected during the tangram task, which might play an essential role in naturalistic visuospatial reasoning.

To test this hypothesis, multivariate Granger causality analysis (GCA) was performed with functional near-infrared spectroscopy (fNIRS) data to characterize the directional FC between various regions of interest (ROIs).[7,8] GCA offers the potential for inferring causal interactions between the various ROIs.[9] More specifically, multivariate GC is also called conditional GC, which is increasingly being applied to functional imaging data to construct the effective brain networks. Meanwhile, fNIRS is an ideal neuroimaging tool for the investigation of cognition and brain disorders because of its unsurpassed advantages including fewer body constraints[10-15], simplicity of use in ecologically valid environments, and noninvasive nature. In this study, the fNIRS neuroimaging technique was utilized to measure the hemoglobin changes in the bilateral prefrontal cortex (PFC), AG, and SAC during tangram and control tasks in a natural environment. Consequently, the tangram task can be performed in a natural environment without causing significant motion artifacts for fNIRS recordings. In addition, a traditional spatial reasoning paradigm was also adopted to examine visuospatial reasoning in a restrained environment, which can serve as a contrast test to disclose tangram-elicited brain activation.

In this study, multivariate GCA combined with fNIRS recordings was performed to inspect the difference in causal brain networks between the tangram and spatial reasoning tasks. It is expected that the investigation into the measure of effective connectivity between fronto-parietal networks can pave a new avenue for an improved understanding of the neural mechanisms underlying spatial reasoning in a natural environment.

2. Materials and Methods

Participants

Twenty-nine right-handed college students aged 18 to 25 (mean age = 21.1, 15 females and 14 males) participated this experiment. All participants had normal or corrected-to-normal vision and had no histories of neurological or psychiatric diseases. The protocol for the present study was approved by the Ethics Committees of the University of Macau.

Procedures and Materials

The schematic of the present stimuli task in a natural environment was illustrated in Figure 1 (1A~1D). Participants were instructed to perform two tasks: a tangram task and a spatial reasoning task.

The tangram task consisted of two conditions: the tangram condition, which required participants to determine how to solve a tangram, and the match condition, in which seven pieces of puzzles were explicitly illustrated, and the participants needed to assemble them accordingly. For the tangram task, the match case served as the control condition to rule out the possible influence of motion, whereas the tangram case served as the experimental condition. The blocked-based paradigm had six blocks for the tangram and match condition, respectively. In particular, the tangram task started with the match block and was performed in an ABBA order for both the tangram and match blocks, respectively.

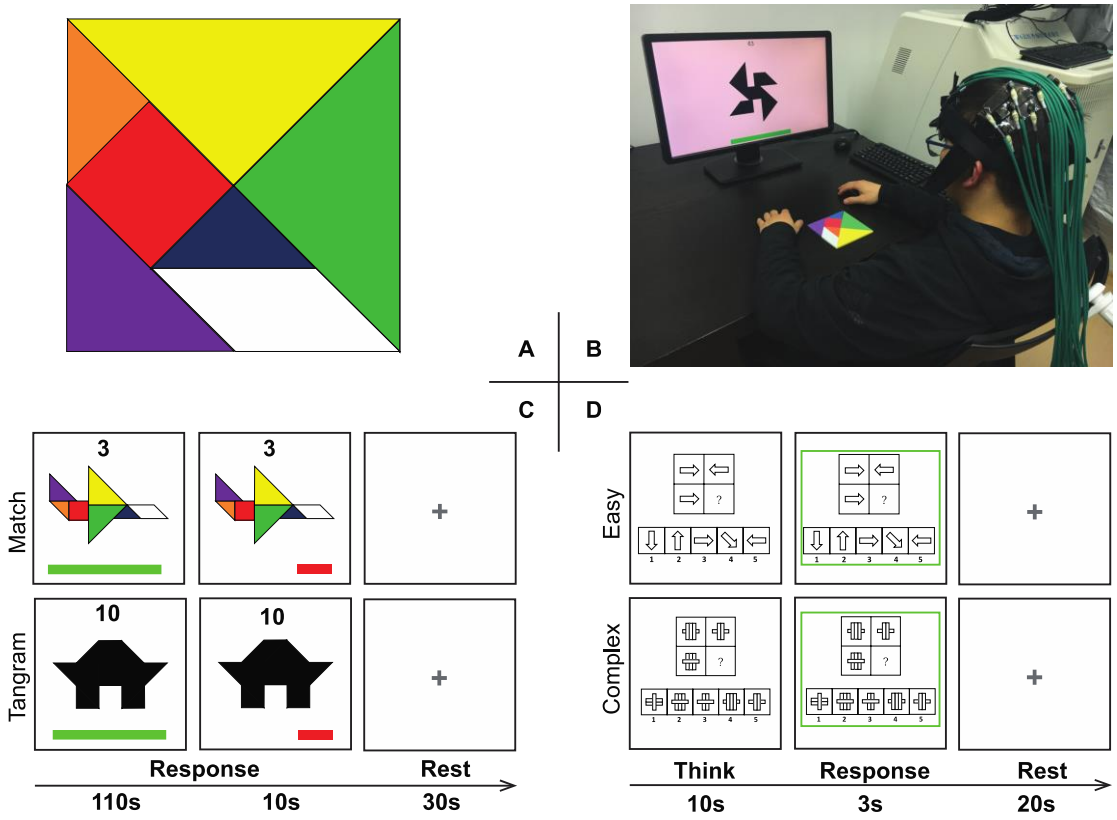

Figure 1 Schematic representation of the experimental protocol. (A) Original tangram set. (B) Experimental scenario. (C) The tangram task, which consisted of the match (top) and tangram (bottom) conditions. In each task block, the participants were given 2 min to solve a randomly presented tangram or to match the given structure. Once the tangram was correctly solved or the structure was correctly matched, the next stimulus would be presented. There was a green progress bar at the bottom indicating the remaining time, which would turn red when only 10 s were left, and a number on the top of the screen indicating the reference number of the shape for participants to check. After 2 min, a gray fixation cross was displayed in the center of the screen for 30 s, indicating the rest period. (D) The spatial reasoning task, which consisted of the simple (top) and complex (bottom) conditions. Participants were given 10 s to think and another 3 s to respond by pressing a number between 1 and 5 when a green rectangle was presented as a cue. After that, a gray fixation cross was displayed in the center of the screen for 20 s, during which the participants were allowed to rest and prepare for the next trial.

By contrast, the stimuli materials for the spatial reasoning task were extracted from the matrix reasoning subtests of the Wechsler Adult Intelligence Scale,[16] which was used to assess the inductive spatial reasoning. The spatial reasoning task also had two conditions: the simple (control) condition, which involved only one change in the size, shape, rotation or position of a picture, and the complex (experimental) condition, which involved two changes of the picture. Different from the tangram task, the spatial reasoning task adopted an event-related paradigm, which consisted of 60 random trials with 30 trials for each condition.

fNIRS Data Acquisition and Pre-processing

fNIRS signals were collected using a CW6 fNIRS system (TechEn Inc., Milford, MA) with a sampling rate of 50 Hz. Eight laser sources and 16 detectors were individually placed into the holes distributed along a homemade patch with a fixed 3 cm interoptode distance. After the experiment, the 3D positions of the optodes were measured by a three-dimensional digitizer (PATRIOT, Polhemus, Colchester, Vermont, USA). Then the grand-averaged coordinates were processed by NIRS-SPM to estimate the Montreal Neurological Institute (MNI) coordinates and associated brain regions of the optodes and channels. Subsequently, the optodes and channels were visualized by BrainNet Viewer (http://www.nitrc.org/projects/bnv/) according to their MNI coordinates. The brain region corresponding to each channel was displayed in Figure 2.

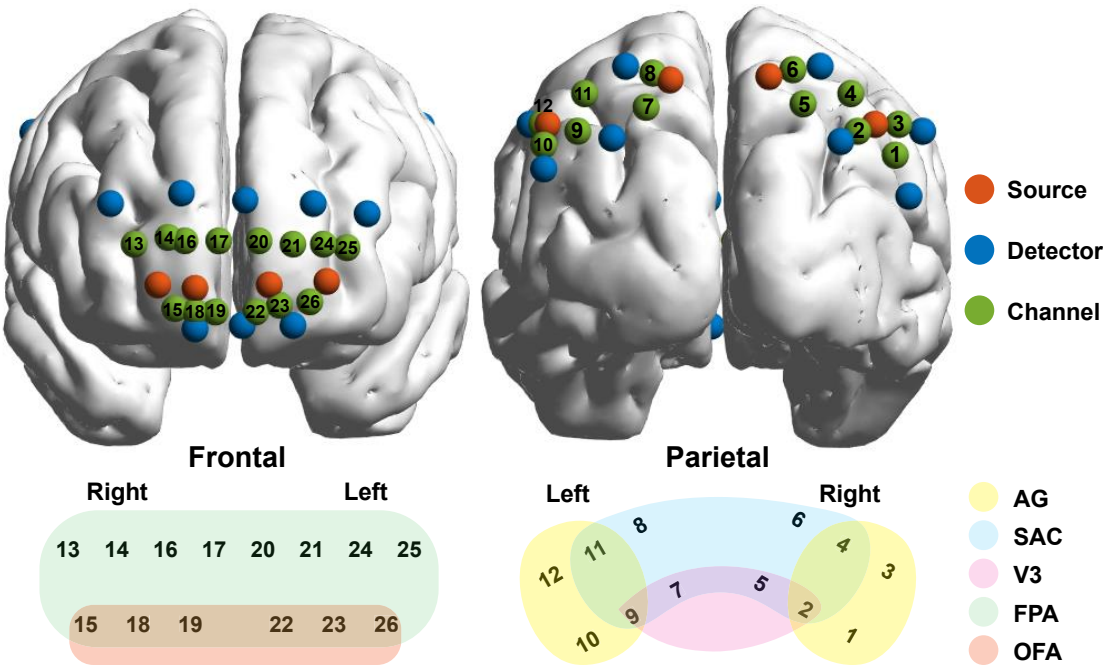

Figure 2 Configuration of the optodes and channels. The sources (red), detectors (blue), and channels (green) are visualized on the brain templates in the first row. Meanwhile, the channels and their associated brain regions are visualized in the second row with different colors indicating different brain regions. AG denotes the angular gyrus, part of Wernicke's area, SAC denotes the somatosensory association cortex, V3 denotes the visual area 3, FPA denotes the frontopolar area, and OFA denotes the orbitofrontal area.

The fNIRS signals were preprocessed with the Homer2 software (Huppert et al., 2009). Similar to previous studies, the raw fNIRS signals were first converted to optical density change data. Then a principal component analysis (PCA) was performed to remove the eigenvectors accounting for 80% of the variance in optical density change data, which were mainly contributed by heart rate and blood pressure oscillations. After the motion artifacts were removed by using a spline method, the signals were filtered with a low-pass filter of 0.2 Hz and then converted to oxyhemoglobin (HbO) and deoxyhemoglobin (HbR) concentration changes. In addition, the concentration changes were normalized by subtracting the mean channel-wise concentration and then divided by the standard deviation (z-scores). Further, the data segmentation was performed, in which each trial consisted of a fixed 2s pre-stimulus period, a 2 min or 13 s duration for the stimulus presentation of the tangram or spatial reasoning task, and then 28 s or 18 s of rest for the tangram or spatial reasoning task, respectively.

Brain Activation

After preprocessing, the grand-averaged z-scores for each condition of each task were calculated across all participants. In particular, the mean z-scores during the stimulus period were calculated for each channel to indicate the brain activation. In this study, only HbO data were analyzed since it has been suggested that HbO signals exhibit a superior signal-to-noise ratio.

Multivariate Granger Causality Analysis

GCA was performed to characterize the directional FC. Specifically, the HbO signals were first downsampled to 2 Hz to ensure a reasonable model order for autoregressive modeling . Then, the regions of interest (ROIs) were identified for the two tasks according to functional connectivity analysis, in which the Pearson correlation between any pair of channels was calculated and grand-averaged after Fisher's r-to-z transformation The average z-score matrixes were then transformed back to the r-value matrixes and were displayed in Figure 3, in which six clusters were clearly identified: the bilateral AG (left: channels 9~12; right: channels 1~4), SAC (left: channels 7 and 8; right: channels 5 and 6), and PFC (left: channels 20~26; right: channels 13~19). The identified ROIs were also consistent with the configurations of the channels in Figure 2.

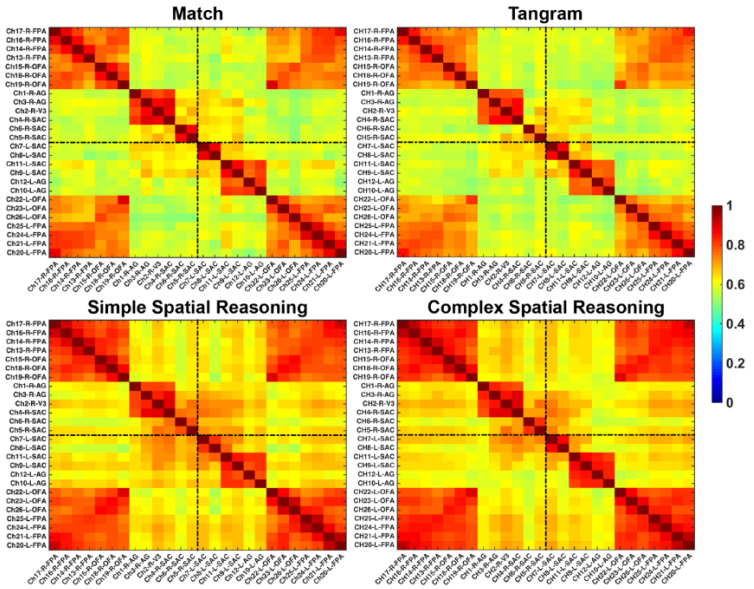

Figure 3 Grand-averaged FC matrixes. A brighter color denotes stronger FC and the channels are labeled in the format of *"channel-hemisphere-brain region"*.

In addition, the fNIRS signals of all channels within each ROI were averaged to generate the time series of each ROI. In consideration of the stationarity of time series, the temporal mean from each trial was removed, and the generated data were further processed by dividing by the temporal standard deviation. The same operation was also performed for the ensemble mean and associated standard deviation.

Further, conditional GCA was conducted using the MVGC, a free MATLAB toolbox with superior computational accuracy and statistical power. Specifically, assuming that *X* and *Y* are the time series of two ROIs, and the time series *Z* with the same length from the other ROIs also imposes causal influences on *X* and *Y*, the value of *X* or *Y* at time point *t* can be predicted by previous *k* time points with a bivariate autoregressive model,

$$X_t = \sum_{i=1}^{k} a_i X_{t-i} + \sum_{i=1}^{k} c_i Z_{t-i} + e_{xt} \quad \text{(Eq. 1)}$$

$$Y_t = \sum_{i=1}^{k} b_i Y_{t-i} + \sum_{i=1}^{k} d_i Z_{t-i} + e_{yt} \quad \text{(Eq. 2)}$$

in which *k* denotes the model order which is determined by Bayesian information criterion and the residuals e_{xt} and e_{yt} denotes the prediction error of the two models, respectively.

If *Y* reduces the variance in the prediction error of *X* when the effect from all other variables *Z* is also considered in the regression model, it is indicated that *Y* GC-causes *X* (vice versa for the case that *X* GC-causes *Y*),

$$Y_t = \sum_{i=1}^{k} b_i' Y_{t-i} + \sum_{i=1}^{k} a_i' X_{t-i} + \sum_{i=1}^{k} c_i' Z_{t-i} + e_{xyt} \quad \text{(Eq. 3)}$$

$$X_t = \sum_{i=1}^{k} b_i'' Y_{t-i} + \sum_{i=1}^{k} a_i'' X_{t-i} + \sum_{i=1}^{k} c_i'' Z_{t-i} + e_{yxt} \quad \text{(Eq. 4)}$$

And then the GC is determined by the comparison between the variance of prediction errors. In particular, the mathematical definition of GC is the logarithm of ratio of the error variances:

$$GC_{(X\to Y)} = \ln\frac{cov(e_{yt})}{cov(e_{xyt})} \quad \text{(Eq. 5)}$$

$$GC_{(Y\to X)} = \ln\frac{cov(e_{xt})}{cov(e_{yxt})} \quad \text{(Eq. 6)}$$

Statistical Analysis

Behavioral performances were assessed by the averaged number of successful trials for the tangram task and by the mean accuracy for the spatial reasoning task. The difference between any two conditions for each task was examined by paired *t*-tests for both behavioral performance and brain activation. Meanwhile, to inspect the role of the frontal and parietal regions during the tangram or spatial reasoning task, a 2 (conditions) by 2 (regions) repeated measure analysis of variance (ANOVA) was performed for each task. In addition, a 2 (tasks: the tangram case vs. the complex reasoning case) by 2 (brain regions: frontal cortex vs. parietal cortex) repeated measure ANOVA was conducted to inspect the interaction between the task and the brain region.

More importantly, a bootstrap method was used to determine the temporal relationships across lags. The time series in each trial were randomly but synchronously shuffled 1000 times and were subjected to GCA. Such procedure can reveal the temporal relationships across lags. Hence, a larger portion of the iterations lower than the GC generated from the original data (which will be referred to as GC values) denotes a stronger directional influence beyond the temporal correlations. Additionally, paired *t*-tests were performed on the GC values for different tests cases.

3. Results

Behavioral Results

The behavioral results were displayed in Figure 4. And we discovered from Figure 4 that participants exhibited better performance for the match condition as compared to that from the tangram condition ($p < 0.001$), and also better performance for the simple condition as compared to that from the complex condition ($p < 0.001$).

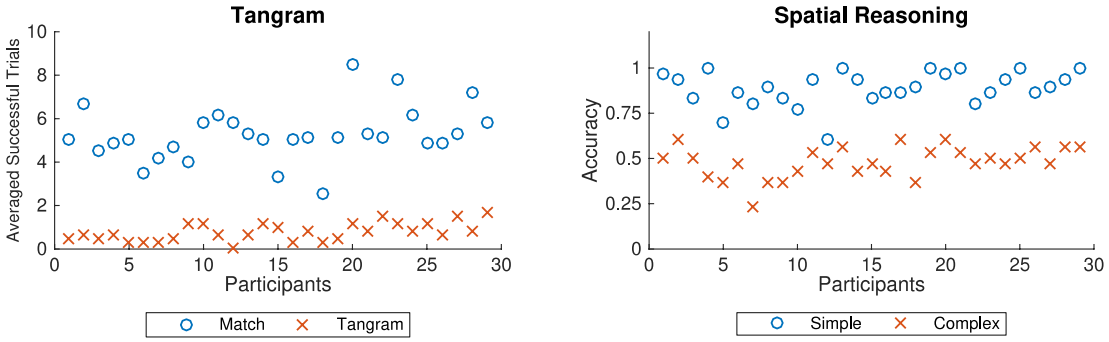

Figure 4 Distributions of the behavioral performance across 29 participants.

Brain Activation

The *t* values were mapped by using the brain cortex template, which were provided in Figure 5(A). It was discovered from Figure 5(A) that the tangram condition exhibited significantly enhanced activation in the prefrontal cortex as compared to the match condition (for all channels, $p < 0.001$). Meanwhile, the tangram condition also showed significant activation in several channels in the bilateral AG (Channels 3, right: $t(28) = 2.74$, Cohen's $d = 0.40$, $p = 0.01$; Channels 10, left: $t(28) = 2.42$, Cohen's $d = 0.41$, $p = 0.02$). By contrast, the complex spatial reasoning condition only exhibited higher brain activation in the right AG (Channel 3, $t(28) = 2.68$, Cohen's $d = 0.50$, $p = 0.01$) and left orbitofrontal area (Channel 26, OFA; $t(28) = 2.52$, Cohen's $d = 0.50$, $p = 0.02$) as compared to the simple condition.

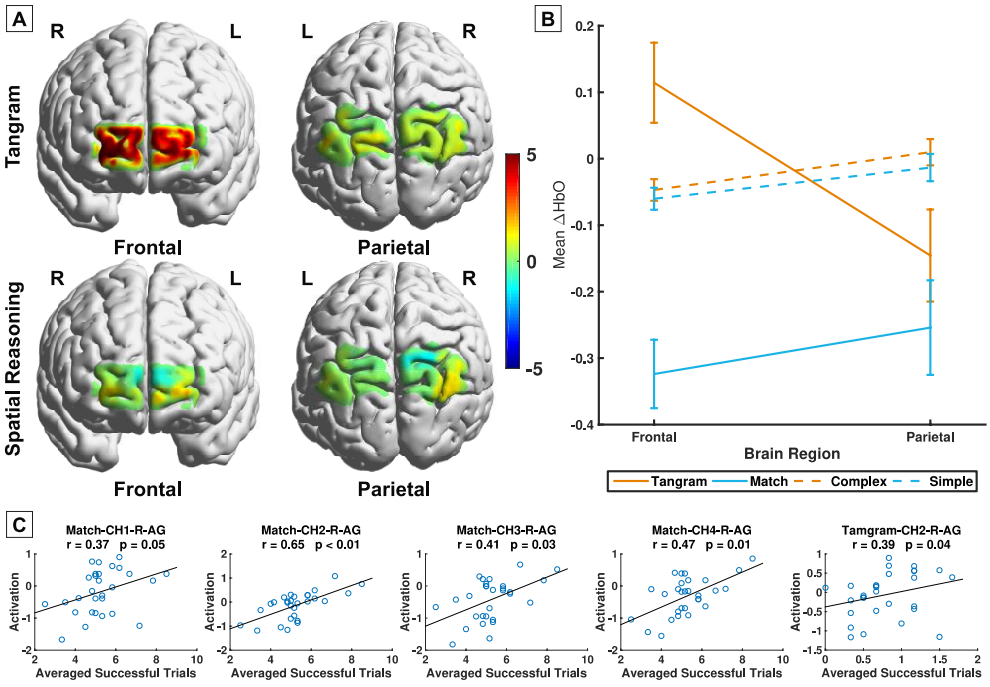

Figure 5 Brain activation and its relationship with behavioral performance. (A) *T*-maps on the brain templates. A brighter color in the T-maps denotes higher *t* values from the *t*-tests. (B) Line chart of the averaged concentration. (C) Scatter plots of the significant correlations.

Additionally, a repeated measure ANOVA was performed to reveal the interaction between the condition and activation in various brain regions. The grand-averaged HbO concentrations and their variance were provided in Figure 5(B) for different test cases. The ANOVA results demonstrated that the tangram task exhibited a main effect of condition ($F(1,28) = 36.64$, $p < 0.001$, $partial\ \eta^2 = 0.57$). In addition, the interaction between the condition and region was also significant ($F(1,28) = 36.61$, $p < 0.001$, $partial\ \eta^2 = 0.57$). Further post hoc analysis showed that for both the parietal and frontal regions, the tangram condition induced enhanced activation ($P_{\text{Bonferroni}} < 0.001$) as compared to the match condition. However, the tangram condition exhibited higher activation in the frontal cortex than that in the parietal cortex ($P_{\text{Bonferroni}} = 0.007$).

By contrast, the ANOVA results illustrated that the spatial reasoning task exhibited a main effect of region ($F(1,28) = 9.34$, $p = 0.005$, $partial\ \eta^2 = 0.25$), in which significantly high brain activation was identified in the parietal cortex ($p = 0.005$). However, the main effect of condition or interaction between the condition and region was not significant for the spatial reasoning task.

Likewise, the ANOVA was also performed to inspect the interaction between the experimental case (tangram case vs. complex spatial reasoning case) and brain region (frontal vs. parietal cortex). We discovered that although no main effect was detected, the experimental case and region showed significant interaction ($F(1,28) = 14.03$, $p < 0.001$, $partial\ \eta^2 = 0.33$). For example, compared to the complex spatial reasoning case, the tangram case exhibited enhanced activation in the frontal cortex ($p = 0.02$) and decreased activation in the parietal cortex ($p = 0.02$) although the tendency was not significant after Bonferroni correction. It should be noted that the different task design for spatial reasoning and tangram tasks might generate some effect on the brain activation difference between them. Therefore, further investigation should be performed in the future to resolve this issue.

Further, we performed Spearman correlation analysis to examine the relationship between the behavioral performance and brain activation. Since the averaged successful trials of tangram condition were not normally distributed, Spearman rather than Pearson correlation analysis method was used for the present work. It was discovered from Figure 5(C) that activation in the right AG showed positive correlation with the behavioral performance for both conditions of the tangram task. However, this is not the case for spatial reasoning task, in which no significant correlation was detected for both conditions.

Effective Connectivity

The GCA results were visualized in matrix form, as plotted in Figure 6A. The GC values larger than 93% were also displayed in Figure 6B, in which various effective connectivity networks were constructed for the four cases (two conditions vs. two tasks). Interestingly, for the tangram task, only effective connectivity between the bilateral PFC was identified for the match condition, whereas additional directional connectivity from the left AG to left SAC as well as from the right AG to right SAC were also detected for the tangram condition.

Interestingly, for the spatial reasoning task, the simple spatial reasoning condition exhibited effective connectivity from the right AG to both right SAC and left AG, and also the bidirectional effective connectivity between the bilateral PFC as well as between the left AG and left SAC. By contrast, besides bidirectional effective connectivity between the bilateral PFC, a strong directional connectivity from the right PFC to left AG was discovered for the complex reasoning case although no effective connectivity was detected within the parietal region.

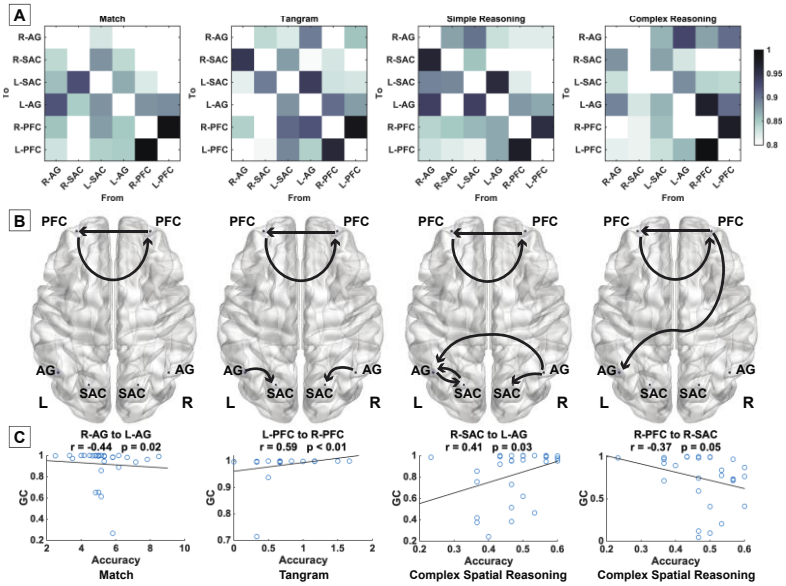

Figure 6 Effective connectivity and its relationship with the behavioral performance. (A) The darker colors denote greater GC values. (B) Effective connectivity with GC values larger than 93%. The arrows denote the direction of information flow. (C) Scatter plots of the significant correlations.

In addition, paired *t*-tests were performed on the GC values for each task to quantify the differences in effective connectivity. We discovered that the tangram condition exhibited enhanced connectivity from the right AG to right SAC ($t(28) = 2.26$, $p = 0.032$, Cohen's $d = 0.60$) than the match condition. By contrast, the complex spatial reasoning condition exhibited enhanced connectivity from the right PFC to left AG ($t(28) = 2.20$, $p = 0.036$, Cohen's $d = 0.55$) and decreased connectivity from the right AG to right SAC ($t(28) = -2.58$, $p = 0.015$, Cohen's $d = -0.56$) as compared to the simple condition.

Further, Spearman correlation analysis was also conducted to detect the relationship between the behavioral performance and effective connectivity. It was discovered from Figure 6(C) that for the match condition, the effective connectivity from the right AG to left AG showed negative correlation with the accuracy, whereas the connectivity from the left PFC to right PFC exhibited positive relationship with the accuracy for the tangram condition. Meanwhile, for the complex spatial reasoning condition, positive correlation was identified between the accuracy and connectivity from the right SAC to left AG, whereas negative correlation was detected between the accuracy and connectivity from the right PFC to right SAC. However, this is not the case for the simple spatial reasoning condition, in which no significant correlation was identified.

4. Discussion

To the best of our knowledge, this is the first study that used fNIRS and GCA to explore the directional FC of the fronto-parietal networks during visuospatial reasoning in a natural environment. We first inspected and compared the behavioral performance and cortical activation between the two conditions for both tangram and spatial reasoning tasks. And then the interactions between the various experimental test cases and brain activation regions were also carefully examined to detect the significant differences between different tests cases. Further, GCA was performed to construct the functional causal networks for each condition of each task.

Although participants showed better behavioral performance for the control conditions than that from the experimental conditions for both tasks, the neural activity in the fronto-parietal regions exhibited significant difference between the two conditions of each task. For example, the complex condition of spatial reasoning task showed enhanced activation in the right AG and left OFA as compared to the simple condition. By contrast, for the tangram task, the match condition manifested decreased activation in both the frontal and parietal cortex than the tangram condition. In particular, we also discovered that the tangram condition exhibited significantly higher activation in the frontal cortex as compared to that in the parietal cortex. However, this is not the case for both conditions in the spatial reasoning task.

The neuroimaging results demonstrated that because participants only needed to match the tangram piece by piece without strongly involving reasoning engagement, the match condition showed decreased activation in both the frontal and parietal cortex. In addition, it is widely recognized that the function of frontal cortex is essential for monitoring process while the parietal cortex is involved in spatial reasoning. As naturalistic spatial reasoning demanded more involvement of the frontal than the parietal cortex, monitoring and planning rather than spatial reasoning were more essential for the tangram condition. Further, as the frontal cortex is closely related to the creative thinking, our finding also demonstrated that the tangram task might measure a different aspect of visuospatial reasoning ability. Unlike the spatial reasoning task, the tangram task does not require participants to figure out a common pattern (inductive reasoning) regarding the changes in size, shape, rotation or position. Such puzzle-solving skills of tangram task might involve more error-and-trial strategies and creative thinking than inductive reasoning of spatial reasoning task. More interestingly, the behavioral performance showed positive correlation with activation in the right AG for both conditions of the tangram task, which phenomenon was not detected for the spatial reasoning task. Consequently, the performance of the visual spatial task, particularly the one requiring matching shapes might be regulated by the activation in right AG, which is critical for spatial cognition.

In addition, distinct causal networks were detected for each condition of the two tasks. For the tangram task, no effective connectivity was identified in parietal cortex for the match condition, which further confirmed that no spatial reasoning involved this case. However, effective connectivity from the bilateral AG to ipsilateral SAC was clearly detected for the tangram condition. Interestingly, the frontal cortex exhibited no directional FC with parietal cortices during the tangram task, which demonstrated that the hands-on experience during the tangram task relieves the demands of consistent monitoring and regulation from the frontal cortex to the parietal cortex. In education practice, such hands-on experiences are essential for children's better understanding of geometry and spatial sense, which requires less cognitive efforts than mental representations.

Further, with increased difficulty, the complex spatial reasoning condition exhibited enhanced effective connectivity from the right PFC to left AG and decreased one from the right AG to right SAC as compared to simple spatial reasoning condition. Thus, it is implied that the fronto-parietal connectivity was more specific to the task difficulty in inductive spatial reasoning, which was also in line with previous studies. Our new results also demonstrated that compared to the simple spatial reasoning, the complex spatial reasoning exhibited enhanced influence from the right to left AG.

In summary, the present study examined the causal networks associated with tangram by using a naturalistic visuospatial reasoning task. More importantly, the high tolerance of body movements of fNIRS made it possible to inspect the neural activity during the tangram task. It was discovered that increased activation in the fronto-parietal regions during the tangram condition and decreased fronto-parietal effective connectivity during the tangram task demonstrated that the tangram task might involve

visuospatial reasoning in a different way from the inductive reasoning. Therefore, the tangram task can be used as a supplement to but not as a substitution of the traditional spatial relation reasoning training in visuospatial education practice.

Acknowledgments

This study was supported by MYRG 2019-00082-FHS and MYRG 2018-00081-FHS grants from the University of Macau, and FDCT 0011/2018/A1 and FDCT 025/2015/A1 grants from Macau government.

References

[1] Ayaz H, Shewokis PA, Izzetoğlu M, Çakir MP, Onaral B. Tangram solved? Prefrontal cortex activation analysis during geometric problem solving. Proc Annu Int Conf IEEE Eng Med Biol Soc EMBS 2012:4724–4727 (2012).

[2] Çakır MP, Ayaz H, İzzetoğlu M, Shewokis PA, İzzetoğlu K, Onaral B. Bridging Brain and Educational Sciences: An Optical Brain Imaging Study of Visuospatial Reasoning. Procedia - Soc Behav Sci 29:300–309 (2011).

[3] Vakhtin AA, Ryman SG, Flores RA, Jung RE. Functional brain networks contributing to the Parieto-Frontal Integration Theory of Intelligence. Neuroimage 103:349–354 (2014).

[4] Newman SD, Carpenter PA, Varma S, Just MA. Frontal and parietal participation in problem solving in the Tower of London: fMRI and computational modeling of planning and high-level perception. Neuropsychologia 41:1668–1682 (2003).

[5] Wendelken C, Ferrer E, Whitaker KJ, Bunge SA. Fronto-Parietal Network Reconfiguration Supports the Development of Reasoning Ability. Cereb Cortex 26:2178–2190 (2016).

[6] Wendelken C, Ferrer E, Ghetti S, Bailey SK, Cutting L, Bunge SA. Frontoparietal Structural Connectivity in Childhood Predicts Development of Functional Connectivity and Reasoning Ability: A Large-Scale Longitudinal Investigation. J Neurosci 37:8549–8558 (2017).

[7] Yuan Z. Combining independent component analysis and Granger causality to investigate brain network dynamics with fNIRS measurements Biomed Opt Express 4:2629 (2013).

[8] Hu Z, Lam K, Xiang Y, Yuan Z. Causal Cortical Network for Arithmetic Problem- Solving Represents Brain ' s Planning Rather than Reasoning. Int J Biol Sci 15:1148–1160 (2019).

[9] Ding M, Chen Y, Bressler SL. Granger Causality: Basic Theory and Application to Neuroscience. Handb Time Ser Anal Recent Theor Dev Appl:437–460 (2006).

[10] Yuan Z, Ye J. Fusion of fNIRS and fMRI data: identifying when and where hemodynamic signals are changing in human brains. Front Hum Neurosci 7:676 (2013).

[11] He Y, Wang M-Y, Li D, Yuan Z. Optical mapping of brain activation during the English to Chinese and Chinese to English sight translation. Biomed Opt Express 8:5399 (2017).

[12] Ieong HF, Yuan Z. Emotion recognition and its relation to prefrontal function and network in heroin plus nicotine dependence: a pilot study. Neurophotonics 5:1 (2018).

[13]X Lin, VLC Lei, D Li, Z Hu, Y Xiang, Yuan, Zhen. Mapping the small-world properties of brain networks in Chinese to English simultaneous interpreting by using functional near-infrared spectroscopy. Journal of Innovative Optical Health Sciences 11(3): 1840001 (2018).[14]

[14] FM Lu, YF Wang, J Zhang, HF Chen, Yuan, Zhen. Optical mapping of the dominant frequency of brain signal oscillations in motor systems. Scientific Reports 7 (1), 14703 (2017).

[15] X Lin, VLC Lei, D Li, Yuan, Zhen. Which is more costly in Chinese to English simultaneous interpreting, "pairing" or "transphrasing"? Evidence from an fNIRS neuroimaging study. Neurophotonics 5 (2): 025010 (2018).

[16] Wechsler D CD& RS. Wechsler Adult Intelligence Test. Psychol Corp (2008).